ELSEVIER

Polymer 42 (2001) 9051–9058

polymer

www.elsevier.com/locate/polymer

Orientation and relaxation of orientation of amorphous poly(ethylene terephthalate)

A. Karim Oultache, Xiaohua Kong, Christian Pellerin, Josée Brisson, Michel Pézolet, Robert E. Prud'homme*

Department of Chemistry and Centre de recherche en sciences et ingénierie des macromolécules, Laval University, Québec, Canada G1K 7P4

Received 12 March 2001; received in revised form 25 April 2001; accepted 25 April 2001

Abstract

Poly(ethylene terephthalate) (PET) has been uniaxially stretched at different draw ratios and draw rates above its glass transition temperature, in the 80–105°C temperature range. Molecular orientation and relaxation have been followed by birefringence. A decrease in temperature reduces the mobility of the oriented chains resulting in a slow relaxation while an increase in stretching rate results in higher orientation values and rapid relaxation after the extension. The same relaxation behavior has been observed from birefringence and polarization modulation infrared spectroscopy. Rouse relaxation times have been estimated from rheological master curves and birefringence relaxation data, while retraction and the reptation times have been deduced from the scaling laws proposed by Doi and Edwards. © 2001 Published by Elsevier Science Ltd.

Keywords: Poly(ethylene terephthalate); Orientation; Relaxation

1. Introduction

The deformation of a viscoelastic material near the rubbery plateau is followed by molecular relaxation. Based on the tube concept, Doi and Edwards have postulated the presence of three relaxation steps [1]. The first one corresponds to a Rouse-like relaxation between entanglements in order to re-establish a constant chain density; it is followed by a relaxation which is associated with the chain retraction inside the deformed tube; the third step corresponds to the chain disengagement from the tube by a reptation process. These steps are characterized by relaxation times τ_a, τ_b, and τ_c.

The validity of this model has been experimentally tested on homopolymers, copolymers, and blends by different groups [2–8]. Tassin and Monnerie [2] have studied the relaxation of polystyrene (PS) of different molecular weights, using infrared linear dichroism, and they have applied the time–temperature superposition principle to obtain master curves of the relaxation data. Thus, they have indirectly shown that the polymer molecular weight does not intervene in the Rouse relaxation step, but that it affects the retraction and reptation times. In our group, Messé et al. [3,4] have studied the relaxation of PS and of polystyrene/poly(2,6-dimethyl 1,4-phenylene oxide) (PS/PPO) blends by means of birefringence and polarization modulation infrared linear dichroism. They have directly determined relaxation times associated with the Rouse and retraction steps, over a wide range of temperatures. These results are in agreement with times determined for PS by Tassin and Monnerie [2], Boué et al. [6], Walczak and Wool [7], and Abtal and Prud'homme [8]. For PS, the reported Rouse times are of the order of 0.5–16 s, and the retraction times of the order of 230–4000 s, depending on temperature, for molecular weights in the 100,000–800,000 range [2,6–8].

The orientation of PET has been intensively investigated in the literature, but fewer studies deal with the relaxation of orientation of this material. Terada et al. [9] and Gupta et al. [10] have studied the crystallization and thermal shrinkage of PET at different temperatures and draw ratios. They have showed that, beyond $\lambda = 3$, PET develops a strain-induced crystallization which impedes the shrinkage and where crystals act as cross-links, preventing the amorphous chain segments from assuming a random coil configuration, in agreement with previous results reported by Nobbs et al. [11]. More recently, Pearce et al. [12] have stretched PET samples at 80°C at different draw rates, quenched them

* Corresponding author. Tel.: +1-418-656-3683; fax: +1-418-656-7916.
E-mail address: robert.prudhomme@chm.ulaval.ca (R.E. Prud'homme).

0032-3861/01/$ - see front matter © 2001 Published by Elsevier Science Ltd.
PII: S0032-3861(01)00397-4

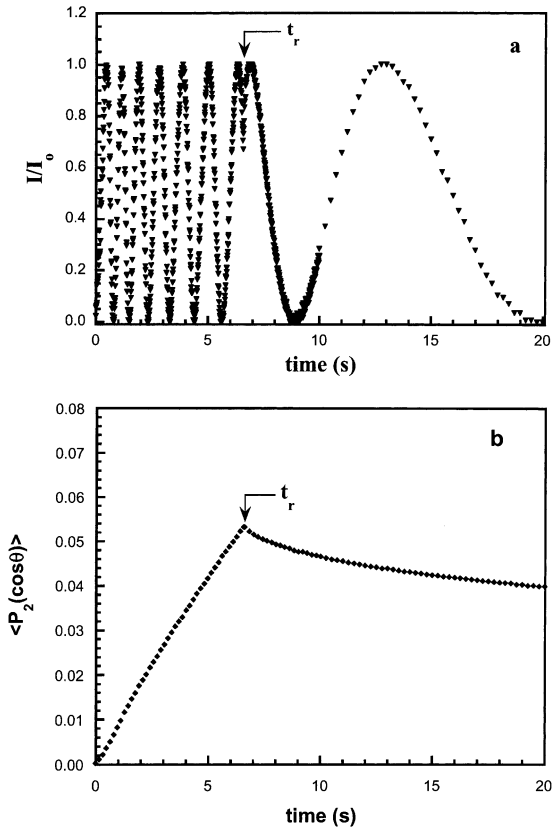

Fig. 1. (a) I/I_0 recorded as a function of time for a PET sample drawn to a λ of 1.5, at 85°C, at a draw rate of 100 mm min^{-1}. (b) $\langle P_2(\cos\theta)\rangle$ of the same sample, as calculated from Eqs. (2)–(4), versus time. Experiments were normally conducted during 3600 s but only the first 20 s are shown here.

immediately after drawing in order to freeze in the orientation, and finally, studied their relaxation by infrared spectroscopy. They have shown that the relaxation is rapid at low λs whereas strain-induced crystallization prevents the PET relaxation when the polymer is stretched at $\lambda \geq 3$.

In this work, measurements of orientation and orientation relaxation of PET have been performed at short and intermediate times, using the birefringence method. They have also been compared with the relaxation curves measured by polarization modulation IR spectroscopy. From the orientation relaxation curves, relaxation times have been directly calculated. In view of the close relationship between chain dynamics and mechanical properties of materials when an imposed deformation is applied, rheological experiments have also been performed. Time–temperature superposition methods, applied to the loss and elastic moduli, have been used to determine molecular parameters such as the molecular weight between entanglements and friction coefficient, and to estimate the Rouse relaxation time. Finally, the retraction and reptation times have been then deduced from the scaling laws proposed by Doi and Edwards and compared to those determined from the orientation relaxation data.

2. Experimental

The commercial films of PET used in this work were purchased from Goodfellow (Cambridge, England). The initial thickness of the films was 0.350 mm for the birefringence, mechanical and infrared measurements, and 1.15 mm for the rheological measurements. They were amorphous, as indicated by X-ray diffraction measurements. They were analyzed with a Perkin–Elmer DSC-7 apparatus at a heating rate of 10°C min^{-1}, and their glass-transition temperature at the middle of the transition was found to be 78°C. Their intrinsic viscosity, in *o*-chlorophenol at 25°C, was found to be 0.80 dl g^{-1}. From the Mark–Houwink relationship established by Aharoni, [13] the number-average molecular weight, M_n, was calculated to be 32,000 g mol^{-1}.

For the birefringence measurements, an apparatus similar to that of Stein et al. [14] has been constructed in our laboratory. It is made of a light beam (5 mW He–Ne laser from Melles Griot, Canada) of wavelength of 632.8 nm that impinges, successively, on the stretched sample and on a beam splitter. Half of the beam is detected by a photodiode located at 90° from the light path, and its intensity is labeled I_0; the second half of the split beam goes through an analyzer and its intensity I is detected by a photodiode placed in the initial beam direction. The incident polarized light and the analyzer are oriented perpendicular to each other and form an angle of 45° with the sample deformation axis. Scattering is reduced by means of a diaphragm placed behind the sample. The detected signals are stored and analyzed. Before positioning the sample, the analyzer is set parallel to the polarized light beam and the two photodiode intensities I_0 and I are adjusted so that they are equal. The 350 μm thick samples were uniaxially deformed using a home-made stretcher at temperatures between 80 and 105°C, at constant rates of 25–100 mm min^{-1}, and at draw ratios (λ) varying from 1.5 to 2.0. λ is here defined as L/L_0, where L and L_0 are, respectively, the initial and final lengths of the deformed sample. The initial sample width and length were, respectively, 5 and 20 mm for all samples. Only stretched samples of high transmittance (70% and more) were considered in this work.

With modern data acquisition systems, birefringence measurements constitute one of the most straightforward methods to evaluate both the orientation and relaxation phenomena of polymers, starting at short times. For an uniaxial deformation of a sample, the birefringence, Δ, is defined as

$$\Delta = n_{\parallel} - n_{\perp} \tag{1}$$

where $n_{\parallel}$ and $n_{\perp}$ are, respectively, the refractive indices parallel and perpendicular to the stretching direction. When a birefringent sample is placed between crossed polarizers, the detected light intensity, I, is given by [15]

$$I/I_0 = \sin^2(\pi\Delta d/\lambda_0) \tag{2}$$

where λ_0 is the wavelength of the incident radiation, and d

the thickness of the sample. Therefore, I/I_0 varies sinusoidally as a function of time as in the example given in Fig. 1a, for a PET sample deformed at 85°C, at a draw ratio of 1.5 and at a stretching rate of 100 mm min^{-1}. Such data were highly reproducible over three samples stretched at the same conditions. As predicted by Eq. (2), each cycle of the curve corresponds to one retardation order. The different orders recorded between zero and time t_r correspond to the increase of the sample molecular orientation during the deformation. At time t_r (Fig. 1a), the deformation is stopped and there is a reversal in the sinusoidal pattern corresponding to the beginning of the relaxation of orientation, following immediately the extension. The subsequent sinusoidal cycles represent the resulting decrease in the orientation due to relaxation. It can be observed in Fig. 1a that the orientation process is rapid as compared to relaxation since the frequency of the I/I_0 oscillations is higher before than after t_r.

In the case of a homogeneous deformation, it can be assumed, as a first approximation, that the sample thickness, d, changes with the draw ratio according to the following equation [16]

$$d = d_0/\lambda^{1/2} \tag{3}$$

where d_0 is the initial sample thickness. Finally, the birefringence of an amorphous polymer is related to the second moment of the orientation function, $\langle P_2(\cos\theta)\rangle$ by [17,18]:

$$\Delta = \Delta_0\langle P_2(\cos\theta)\rangle \tag{4}$$

where Δ_0 is the intrinsic birefringence of the sample, which is equal to 0.275 for amorphous PET [19,20]. The results shown in Fig. 1b indicate that the orientation function increases rapidly and almost linearly with time up to t_r when the deformation of the sample is stopped. From this point, it starts to decrease progressively indicating that relaxation of the orientation occurs.

Measurements of orientation and relaxation were also performed using the polarization modulation infrared linear dichroism (PM-IRLD) apparatus described in Ref. [21], using the same experimental conditions (stretcher, temperature, stretching rate, draw ratio) as for birefringence. This apparatus is made of a Bomem Michelson MB-100 spectrometer, a wire-grid polarizer, a photoelastic modulator and an InSb detector. Usually, the absorption bands at 1340 and 975 cm^{-1}, both associated with the *trans* conformers of the ethylene glycol segment of the repeat unit [22,23], are used to study the orientation and relaxation of PET. In this work, the thickness of the sample did not allow quantitative measurements due to a too high absorption of the infrared beam. However, the band at 3336 cm^{-1} can be used for that purpose, as described in details in a future article [24].

Stress measurements were performed with an Instron model 5565 testing machine equipped with a 5 kg load cell and a home-made environmental chamber. Sample dimensions and stretching conditions (temperature, draw ratio, and stretching speed) were the same as those used in the birefringence measurements.

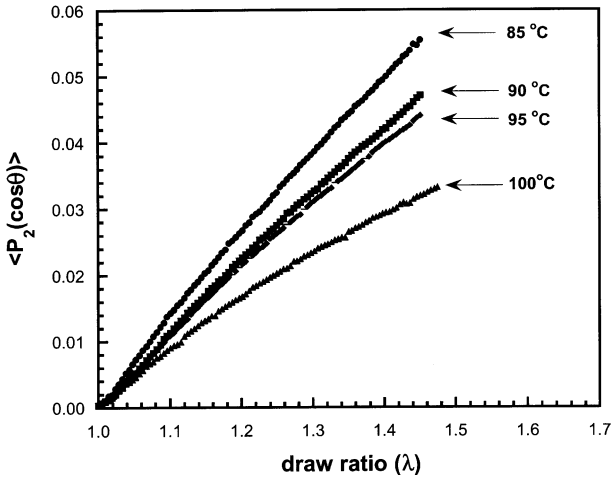

Fig. 2. $\langle P_2(\cos\theta)\rangle$ versus draw ratio during stretching. The draw rate was 100 mm min^{-1}.

For rheological tests, a Bohlin rheometer, equipped with a parallel plate geometry of 25 mm diameter, was used. A disc-shaped PET sample of 1.15 mm in thickness was subjected to an oscillatory stress and the resulting strain was measured. The isothermal evolution of rheological parameters such as storage modulus G' and loss modulus G'' was recorded as a function of frequency ranging from 0.05 to 150 Hz. These measurements were made, every 2.5°, between 80 and 105°C (near the glass transition).

3. Results and discussion

Fig. 2 shows the orientation function versus λ during the deformation of PET samples stretched at a deformation rate of 100 mm min^{-1}, at 85, 90, 95 and 100°C. As can be seen, there is a non-linear increase of $\langle P_2(\cos\theta)\rangle$ with λ and the curvature becomes more pronounced as the temperature is raised, indicating that there is more

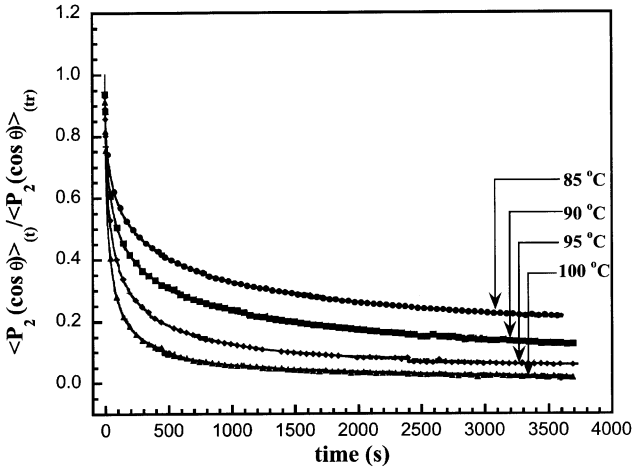

Fig. 3. Normalized PET relaxation curves versus time at different temperatures. Samples were stretched at a draw rate of 100 mm min and $\lambda = 1.5$.

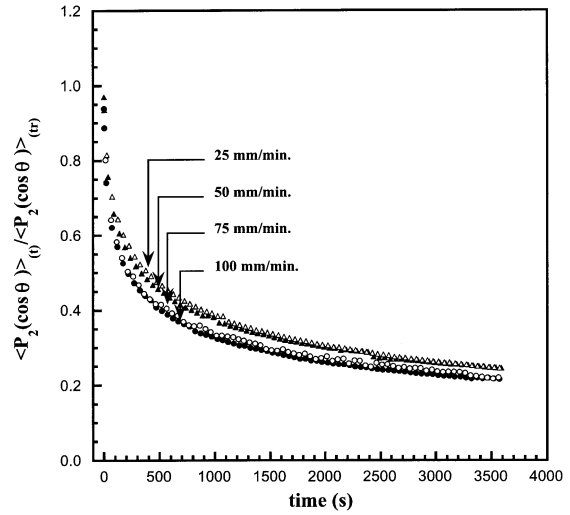

Fig. 4. Normalized PET relaxation curves versus time at different draw rates. Samples were stretched at 85°C and $\lambda = 1.5$.

relaxation. The orientation behavior shown in Fig. 2 does not follow the Gaussian network model which predicts an increasing slope in the orientation function plotted as a function of λ, as given by [25]

$$\langle P_2(\cos\theta)\rangle = \frac{1}{5N}\left(\lambda^2 - \frac{1}{\lambda}\right) \tag{5}$$

where N is the number of freely jointed links between network entanglement points. Several authors [9,11,12] have suggested that PET behaves as a rubber-like network when deformed at low to moderate draw ratios ($\lambda \leq 2.5$) but Clauss and Salem [26] have shown that, when relaxation effects during the deformation are important (especially at low draw rates and high temperatures), this model is not applicable.

The relaxation curves, taken after stretching films to t_r, at the same temperatures, are shown in Fig. 3. For easier comparison, these are normalized with respect to the value at $t = t_r$ In all cases, the relaxation is initially rapid as indicated by the sharp drop of $\langle P_2(\cos\theta)\rangle$ at short times, then slows down, to finally reach a quasi-plateau at longer relaxation times. The higher the temperature, the more rapid is the relaxation, which is due to the increase in polymer chain mobility which accelerates the relaxation.

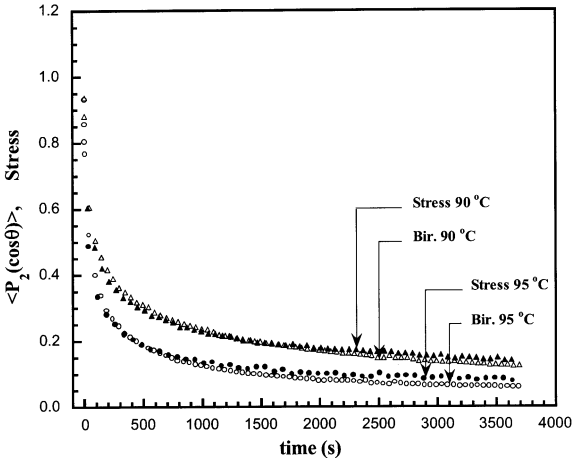

Fig. 5. Relaxation curves of PET samples stretched to $\lambda = 1.5$ at a draw rate of 100 mm min^{-1}, at 90 and 95°C, as measured by birefringence and stress measurements.

Samples stretched to a λ of 1.5 at a slow draw rate (for example 25 mm min^{-1}) in the temperature range of 85–100°C remain amorphous, as indicated by their transmittance which remains above 70%, by the absence of sharp diffraction peaks in X-ray diffraction, by infrared spectroscopy and DSC measurements. When the draw rate is increased to 100 mm min^{-1} (as in Figs. 2 and 3), the samples stretched to a λ of 1.5 at 85°C also remain amorphous, as indicated by the same techniques. In the 90–100°C temperature range, infrared spectroscopy shows a slight increase in the *trans* conformer (1340 cm^{-1} band) with time, DSC shows traces of crystallinity, whereas transmittance (and birefringence) and X-ray diffraction measurements, which are perhaps less sensitive, do not detect any crystallinity. Finally, at higher temperatures (105°C and more), the transmitted intensity decreases to below 25% with time and the birefringence set-up used in this article becomes useless under these conditions, while X-ray diffraction shows the presence of narrow diffraction peaks assigned to the crystalline phase and DSC shows an increase in the degree of crystallinity to about 8%.

Other samples were deformed to $\lambda = 2$ at draw rates varying between 25 and 100 mm min^{-1}, at temperatures between 85 and 100°C. All samples remained transparent (70% transmission or more) and birefringence relaxation measurements (not shown here) were not affected. For example, under the same draw rate and temperature conditions, the normalized relaxation curves obtained at $\lambda = 2$, 1.75 and 1.5 are similar. As expected, at a temperature of 105°C, the sample transmittance dropped to less than 30%, indicating crystallization, as found for $\lambda = 1.5$.

Normalized relaxation curves obtained after stretching samples to $\lambda = 1.5$ at draw rates of 25, 50, 75 and 100 mm min^{-1} are shown in Fig. 4. Immediately after stretching, chains relax faster for higher deformation rates but, at longer times, the difference between these relaxation curves diminishes. Near the rubbery plateau, the polymer orientation involves both a viscous flow due to the slippage of molecules and an elastic chain alignment. Upon deformation, at high stretching rates, the contribution of the viscous flow decreases in favor of the elastic deformation, resulting in higher orientation values; when the deformation is stopped, there is an elastic driving force on the aligned molecules to recover rapidly their initial coiled shape, resulting in a rapid initial relaxation step. Conversely, a low deformation rate increases the chain slippage contribution at the expense of the chain elastic alignment, resulting in low orientation values and in a slower initial relaxation step.

PET samples were also elongated on an Instron machine

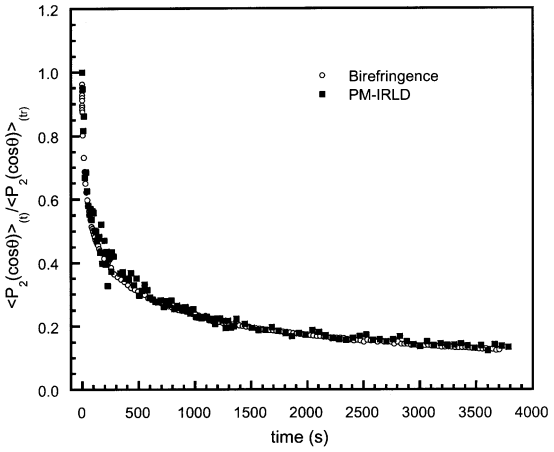

Fig. 6. A comparison of normalized PET relaxation curves obtained by birefringence and PM-IRLD. Samples were stretched at 90°C, at a draw rate of 100 mm min^{-1}, to $\lambda = 1.5$.

to a draw ratio of 1.5, at a rate of 100 mm min^{-1} and at temperatures of 85, 90 and 95°C. The (relative) variation of the stress needed to maintain the deformation is shown in Fig. 5 as a function of time at two temperatures. The results, normalized with respect to the stress measured when the extension is stopped (at $t = t_r$), are compared to those of birefringence obtained under the same deformation conditions. The two sets of results are very similar: the higher the temperature, the lower the stress (or birefringence) and the higher the relaxation rate. Under these conditions, the stress-optical coefficient (SOC) [1,25], which is defined as the ratio of birefringence to true stress, remains almost constant (about 7×10^{-9} Pa^{-1}) over the entire relaxation time at 85 and 90°C, in agreement with the values of 5.5–6×10^{-9} Pa^{-1} reported in the literature [27,28]. As the temperature increases to 95°C, the SOC slightly increases to 10×10^{-9} Pa^{-1} for the first relaxation stage, but diminishes progressively with time to reach the SOC values obtained at the two other temperatures.

Fig. 6 shows the birefringence and PM-IRLD relaxation curves of samples (350 μm in thickness) stretched to a λ of 1.5 at 90°C. Within experimental error, the two curves are similar, including the same limiting values at long times. This is an independent confirmation of the quality of the birefringence relaxation curves recorded in this study.

Table 1
Characteristic data for PET

M_n (g mol^{-1})	32000
M_e (g mol^{-1})	2500
G_n^0 (Pa)	1.5×10^6
$[\eta]$ (dl g^{-1})	0.80
$a^2\xi$ (dyne s cm)	3.88×10^{-14}
C_1^g	8.5
C_2^g (°C)	26
T_g (°C)	78
T_{inf} (°C)	52
T_m (°C)	242

PET has been deformed near its T_g where the chain dynamics are intimately related to the polymer structure as characterized by molecular weight, molecular weight between entanglements and friction coefficient. In this region, Doi and Edwards have postulated that the relaxation is the sum of three processes: Rouse, retraction, and reptation [1]. In this context, the Rouse time, τ_a, is a function of the number of repeat units between entanglements, n_e, as shown by the equation

$$\tau_a = \frac{a^2 \xi (M_e/M_0)^2}{6\pi^2 kT} \tag{6}$$

where M_e is the molecular weight between entanglements, M_0 the repeat unit molecular weight, $n_e = M_e/M_0$, a is the characteristic length of the repeat unit, ξ the friction coefficient, k the Boltzmann constant, and T the temperature. The retraction time, τ_b, is proportional to the square of the chain molecular weight, following the expression

$$\tau_b = 2\tau_a (n/n_e)^2 \tag{7}$$

where n is the number of repeat units per chain defined by M_n/M_0, n_e the number of repeat units between entanglements, and M_n the number-averaged molecular weight. Finally, the reptation time, τ_c, is proportional to the cube of the chain molecular weight, as expressed by

$$\tau_c = 6\tau_a (n/n_e)^3 \tag{8}$$

The determination of τ_a, τ_b, and τ_c using the Doi–Edwards theory requires, therefore, the knowledge of M_e, a and ξ, which can be obtained from rheological measurements (M_n has already been determined from viscosity measurements — see Table 1).

3.1. Determination of Me

Oscillatory shear measurements were performed in the T_g region. The isothermal storage and loss moduli G' and G'' were obtained as a function of frequency. Curves obtained at different temperatures were superposed in the standard manner into respective master curves by the use of the time–temperature superposition principle [29,30]. Horizontal shift factors (a_T) were determined by eye. No vertical shift was used. Fig. 7a shows the master curve of G' and G'' at a reference temperature, T_0, of 85°C. The scatter in G'' at high frequency arises from the fact that, in this region, the data start to deviate from the linear viscoelasticity behavior. In the abscissa, $\log a_T$, which is defined as the shift factor, depends on the temperature through the WLF equation

$$-\frac{(T - T_0)}{\log a_T} = \frac{T - T_0}{C_1^0} + \frac{C_2^0}{C_1^0} \tag{9}$$

where C_1^0 and C_2^0 are two viscoelastic constants at the

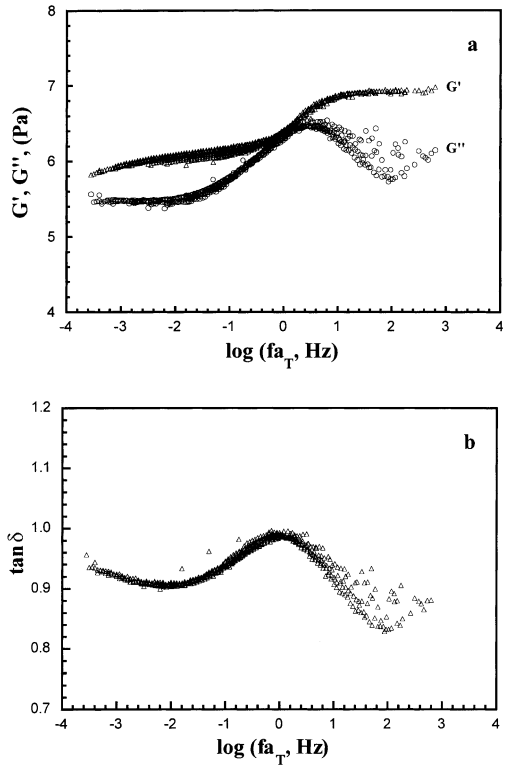

Fig. 7. Master curves at a reference temperature of 85°C for: (a) storage modulus G' and loss modulus G'', (b) tan δ.

reference temperature T_0. These constants can be calculated from the slope and the intercept of the $(T - T_0)/\log a_T$ versus $(T - T_0)$ plot (Eq. (9)), and can be reported to the glass transition temperature (C_1^g and C_2^g), using well known equations [29]. The temperature, T_{inf}, at which the cooperative motions involved in the glass transition would appear at infinitely low frequency, is related to C_2^0 as

$$T_{inf} = T_0 - C_2^0 \tag{10}$$

The values of C_1^g, C_2^g, and T_{inf} were calculated using the usual equations, and the results are reported in Table 1.

The pseudoequilibrium modulus of the entanglement network, G_n^0, is related to the average molecular weight between entanglements through [29]

$$G_n^0 = \frac{g_n \rho RT}{M_e} \tag{11}$$

where g_n is a numerical factor assumed to be unity, R the gas constant, and ρ the density. ρ was calculated to be 1.25 g cm^{-3} at 85°C since it varies from 1.34 at 25°C to 0.989 g cm^{-3} at 275°C [31]. The master curve of tan δ, defined as the ratio of G'' to G', passes through a minimum, as shown in Fig. 7b. The modulus G' at the frequency where tan δ is at its minimum is equal to G_n^0. The values of G_n^0 and M_e calculated from Eq. (11) are 1.5×10^6 Pa and 2500 g mol^{-1}, respectively. Wu has determined for PET a G_n^0 value of 3.1×10^6 Pa at 548 K using an empirical equation which relates the plateau modulus to the crossover modulus and to polydispersity [31]. This value, which is slightly higher than that obtained in this study, leads to an average molecular weight between entanglement of 1450 g mol^{-1}. Lorentz and Tassin [32] have reported a value of M_e of 1200 g mol^{-1} while, from viscosity measurements [13], Aharoni has estimated the critical molecular weight of entanglements M_c (roughly twice M_e) to be about 3500 g mol^{-1}.

3.2. Determination of $a^2\xi$

In the transition region, there is a small frequency range where G' is equal to G'', and both are proportional to the square root of the frequency f (Fig. 7a). According to the Rouse theory, the relaxation times are sufficiently short to allow using the following expression [29,33]

$$G' = G'' = \left(\frac{a\rho N}{4M_0}\right)[\xi kT/3]^{1/2} f^{1/2} \tag{12}$$

where N is the Avogadro number, the other parameters having already been defined. From Eq. (12), it is possible to calculate the product $a^2\xi$ since the values of G' and G'' are known in this region. Another experimental method to determine $a^2\xi$ is to draw two lines of slopes 0 and 1/2 in the plateau and transition zones, respectively, in a double logarithmic plot of G' against frequency. The frequency intersection point, f_{tr}, of the two lines is related to the $a^2\xi$ factor through [29]

$$f_{tr} = \frac{48kT}{a^2(M_e/M_0)^2\xi} \tag{13}$$

Although the plateau of slope 0 is never seen in Fig. 7, the method described by Eq. (13) can still be used in first approximation. The values of $a^2\xi$ calculated from Eqs. (12) and (13) are then in good agreement and only an averaged value is reported in Table 1.

Then, using Eq. (6) and the parameters given in Table 1, τ_a has been calculated to be 2 s at 85°C. On the other hand, Ferry has reported that, according to the Rouse–Moony theory, the onset frequency, f_{tr}, of Eq. (13) is also equal to [29]

$$f_{tr} = 8/\pi^2\tau_{tr} \tag{14}$$

where τ_{tr} is the longest relaxation time in the transition zone. From Eq. (14), τ_{tr} is calculated to be about 2.2 s, in agreement with the above-mentioned value of τ_a. The two other relaxation times τ_b and τ_c deduced from the scaling laws given by Eqs. (7) and (8) are, respectively, 655 s and 420 min.

3.3. Relaxation times derived from birefringence

Since the relaxation of orientation has an exponential form in the Doi–Edwards formulation, relaxation times have been calculated by fitting the birefringence relaxation

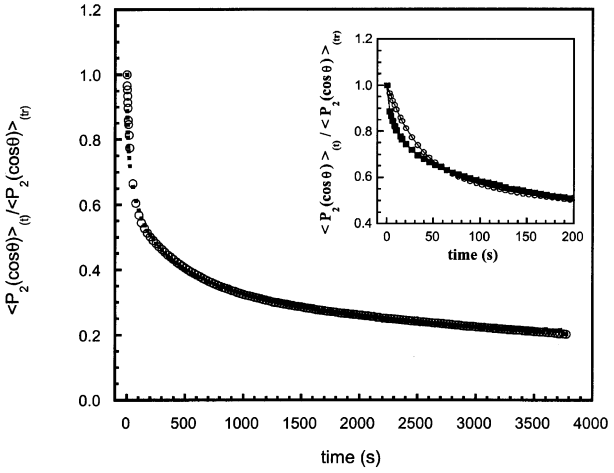

Fig. 8. A comparison of the birefringence experimental (square) and calculated (circle) relaxation curves obtained using Eq. (15) (with $n = 3$). The insert shows an enlargement of the initial portion of the graph (at short times).

curves with exponential equations such as

$$P_2(t) = \sum_{i=1}^{n} A_i \exp(-t/\tau_i) \tag{15}$$

where $P_2(t)$, A_i, and τ_i are, respectively, the orientation function at time t, the pre-exponential factor, and the relaxation time. The use of hyperbolic and stretched exponential functions was eliminated since the first function gives a poor fit with experimental results, while the second predicts a linear relationship in a double logarithmic plot of the orientation versus time, in disagreement with our experimental results. A sum of only two exponential functions also leads to a poor agreement with the experimental results. However, a satisfactory correlation between the experimental and the theoretical curves has been obtained using a sum of three exponential functions ($n = 3$).

Fig. 8 shows a comparison between the experimental birefringence curve and the calculated curve using Eq. (15) with $n = 3$. As shown in the insert, the calculated relaxation curve slightly deviates from birefringence data at short times, where it is systematically above the experimental data. This means that the fitting procedure used slightly overestimates the first relaxation time. The calculated τ_1, τ_2 and τ_3 values thus obtained at 85, 90, 95 and 100°C are shown in Table 2. As expected, these relaxation times decrease when the temperature increases. At 85°C, τ_1 is higher than the Rouse time calculated from rheological data in the previous section but considering the very different origin of these two sets of data, and the overestimation mentioned above, the general agreement found is considered satisfactory. Moreover, it can be argued that the birefringence τ_1 is subjected to a systematic error because the sample deformation was not instantaneous (see Fig. 1) and some relaxation already occurred during this period of time. Finally, it is recognized that rheological measurements were made in the linear viscoelastic regime since the strain imposed on the sample is of the order of 1% whereas the birefringence measurements involve large deformations. In view of this important difference, it may not be surprising to obtain slightly different τ_1 values by these two methods. Experimental errors of the order of ± 5, ± 50, and ± 400 s are estimated for, respectively, τ_1, τ_2, and τ_3, although it is larger than that for τ_3 at 85 and 90°C because the values reported in Table 2 lie outside the range of the experimental measurements.

Table 2
Relaxation times of PET films stretched at $\lambda = 1.5$ and at a draw rate of 100 mm min^{-1}

Temperature (°C)	τ_1 (s)	τ_2 (s)	τ_3 (s)
85	22	366	6830
90	19	320	4550
95	14	222	3120
100	11	144	1910

Birefringence τ_2 and τ_3 values are much smaller than the reptation time (obviously, the relaxation measurements made in this study do not cover the reptation step) but are of the same order of magnitude as the retraction time calculated from rheology data and the scaling law, Eq. (7). It is also noticed that τ_3/τ_1 (from Table 2) and τ_b/τ_a (from Eq. (7)), which equal 310 and 327, respectively, are quite close. The assignment of the experimental relaxation times to the different chain relaxation dynamics modes of PET still need to be done. An attempt has already been made by Messé et al. [3,4] to fit the experimental relaxation curves of PS homopolymers and PS/PPO blends, using similar exponential equations. They have determined three relaxation times τ_1, τ_2, and τ_3 and have associated τ_1 with τ_a, and τ_3 with τ_b in the Doi–Edwards framework, whereas τ_2 has been attributed to a difference in the friction coefficient which may exist between the chain ends and the middle of the chain. Additional measurements need to be done to confirm this interpretation.

4. Conclusions

The orientation and the relaxation of orientation of PET have been determined by birefringence. During the deformation, the orientation increases with the increase of both draw ratio and stretching rate, and decreases with temperature. This is explained by the presence of two competitive phenomena: orientation and relaxation. After the extension, the polymer starts to loose its orientation. An increase in the temperature increases chain mobility, resulting in a rapid relaxation, while an increase in the stretching rate reduces chain slippage to the detriment of the elastic deformation, resulting in high orientation values which relax rapidly after the extension. Relaxation times have been determined from birefringence curves and the shortest one agrees reasonably with the Rouse relaxation times determined by rheological

measurements. Finally, molecular parameters such as PET molecular weight between entanglements and friction coefficient have been determined from rheological master curves.

Acknowledgements

We gratefully acknowledge the Natural Sciences and Engineering Research Council of Canada and the Department of Education of the Province of Québec (FCAR program) for financial support. We would also like to thank Dr Mosto Bousmina for making the Bohlin rheometer available to us.

References

[1] Doi M, Edwards SF. The theory of polymer dynamics. Oxford: Oxford University Press, 1986.
[2] Tassin JF, Monnerie L. Macromolecules 1988;21:1846.
[3] Messé L, Pézolet M, Prud'homme RE. Polymer 2001;42:563.
[4] Messé L, Prud'homme RE. J Polym Sci, Phys 2000;38:1405.
[5] Tassin JF, Monnerie L, Fetters LJ. Macromolecules 1988;21:2404.
[6] Boué F, Nierlich M, Jannink G, Ball RC. J Phys 1982;43:137 [Paris].
[7] Walczak WJ, Wool RP. Macromolecules 1991;24:4657.
[8] Abtal E, Prud'homme RE. Polymer 1993;34:4661.
[9] Terada T, Sawatari C, Chigono T, Matsuo M. Macromolecules 1982;15:998.
[10] Gupta VB, Radhakrishnan J, Sett SK. Polymer 1993;34:3814.
[11] Nobbs JH, Bower DI, Ward IM. Polymer 1976;17:25.
[12] Pearce R, Cole KC, Ajji A, Dumoulin MM. Polym Eng Sci 1997;37:1795.
[13] Aharoni SM. Makromol Chem 1978;179:1867.
[14] Kumar S, Stein RS. J Appl Polym Sci 1987;34:1693.
[15] Stein RS. Rubber Chem Technol 1976;49:458.
[16] Wilkes GL. Macromol Sci Rev Macromol Chem, C 1974;10(2): 149.
[17] Ward IM. Development in oriented polymers. 2nd ed. London: Elsevier Applied Science, 1987.
[18] Samuels R. Structured polymer properties. New York: Wiley, 1974.
[19] Dumbelton JH. J Polym Sci, A 1968;2:6795.
[20] Sun T, Desper CR, Porter RS. J Mater Sci 1986;21:803.
[21] Buffeteau T, Pézolet M. Appl Spectrosc 1996;50:948.
[22] Padibjo SR, Ward IM. Polymer 1983;24:1103.
[23] Ajji A, Guèvremont J, Cole KC, Dumoulin MM. Polymer 1996;37:3707.
[24] Pellerin C, Rousseau ME, Prud'homme RE, Pézolet M. In preparation.
[25] Treloar LRG. The physics of rubber elasticity. 3rd ed. Oxford: Clarendon Press, 1975.
[26] Clauss B, Salem DR. Macromolecules 1995;28:8328.
[27] Long SD, Ward IM. J Appl Polym Sci 1991;42:1921.
[28] Matthews RG, Duckett RA, Ward IM. Polymer 1997;38:4795.
[29] Ferry JD. Viscoelastic properties of polymers. 3rd ed. New York: Wiley, 1980.
[30] Williams ML, Landel RF, Ferry JD. J Am Chem Soc 1955:3701.
[31] Wu S. J Polym Sci Polym Phys Ed 1989;27:723.
[32] Lorentz G, Tassin JF. Polymer 1994;35:3201.
[33] Rouse Jr. PE. J Chem Phys 1953;21:1272.